

RESEARCH PAPERS

Proteomic insights into changes in grapevine wood in response to esca proper and apoplexy

MARYLINE MAGNIN-ROBERT^{1†}, ALESSANDRO SPAGNOLO^{1†}, TCHILABALO DILEZITOKO ALAY², CLARA CILINDRE³, LAURENCE MERCIER⁴, CHRISTINE SCHAEFFER-REISS², ALAIN VAN DORSSELAER², CHRISTOPHE CLÉMENT¹ and FLORENCE FONTAINE¹

¹ Université de Reims Champagne-Ardenne, URVVC EA 4707, Laboratoire Stress, Défenses et Reproduction des Plantes, BP 1039, 51687 Reims Cedex 2, France

² Université de Strasbourg, IPHC, UMR 7178, Laboratoire de Spectrométrie de Masse Bioorganique, 67087 Strasbourg, France

³ Université de Reims Champagne-Ardenne, URVVC EA 4707, Laboratoire d'Œnologie et Chimie Appliquée, BP 1039, 51687 Reims Cedex 2, France.

⁴ Moët & Chandon, 6 rue Croix de Bussy, 51200 Epernay, France

† Contributed equally to the work

Summary. Among fungal grapevine trunk diseases, esca proper poses a significant threat for viticulture. Apoplexy, mainly occurring on grapevines affected by esca proper, is also a threat. To verify if different responses are activated in the woody tissues of apoplectic (A) and esca proper-affected (E) vines, two-dimensional gel electrophoresis coupled to mass spectrometry analysis was used to examine changes in the trunk wood of E and A field-grown plants. Asymptomatic and black streaked trunk (BST) wood from A and E plants were compared to asymptomatic and BST wood of control plants. Twenty-seven differentially expressed protein spots were identified. For eleven targeted proteins, expression of the relative transcripts was also monitored by qRT-PCR. Hierarchical tree clustering revealed differences in the distribution of spots containing carbohydrate metabolism proteins and heat shock proteins between asymptomatic- and BST-wood of grapevine, irrespective of the type of plant examined (control or diseased grapevines). Asymptomatic wood was mainly characterized by down-expression of proteins involved in cell growth and defense responses. The proteome of BST wood, characterized by extensive presence of grapevine trunk disease agents, revealed over-expression of proteins involved in defense. There was no evidence of strong different response in the trunk wood of apoplectic and esca proper affected plants. This could mean that, despite the different feature of these external crown symptoms, grapevine responses at trunk wood level is very similar in both cases. This plant response might therefore either simply be due to the fact that plants can react in the same way to different stresses, or that apoplexy represents a different effect provoked by the same cause or causal agent(s).

Key words: grapevine, proteomics, qRT-PCR, trunk diseases, Chardonnay.

Introduction

Grapevine trunk diseases have increased in incidence over the last 15 years (Fussler *et al.*, 2008; Bertsch *et al.*, 2013) and now pose serious problems for viticulture worldwide (Bertsch *et al.*, 2013). They are caused by fungal pathogens that attack the

woody perennial organs of vines and ultimately lead to vine death. The predominant grapevine trunk diseases are eutypa dieback, botryosphaeria dieback and the esca disease complex. For the latter, five syndromes have been described: brown wood streaking (mostly affecting rooted cuttings), Petri disease, grapevine leaf stripe disease (GLSD), esca and esca proper (Surico *et al.*, 2008; Surico, 2009). GLSD is a widespread tracheomycotic syndrome, for which the major causal agents are *Phaeoemoniella chlamydo-spora* (W. Gams, Crous, M.J. Wingfield & L. Mugnai)

Corresponding author: F. Fontaine
Fax: +33 32 6913339
E-mail: florence.fontaine@univ-reims.fr

P.W. Crous & W. Gams (Pch) and *Phaeoacremonium aleophilum* W. Gams, P.W. Crous, M.J. Wingfield & L. Mugnai (Pal) (Surico *et al.*, 2008). Esca is a typical white decay occurring in the trunks and branches of standing vines, for which the causal agents are different Basidiomycete species represented mainly by *Fomitiporia mediterranea* (Fom) M. Fischer in Europe and the Mediterranean basin (Surico *et al.*, 2008; Surico, 2009). The coexistence of GLSD and esca on the same plant is called esca proper (Surico, 2009). Plants affected by esca proper are thus characterized by wood symptoms comprising several forms of discoloration, among which black streaking involving single or several xylem vessels and areas with darkened or brown necrosis circumscribing the pith are most commonly observed.

Additionally, symptoms on leaves can emerge. These are typically characterized by spots appearing between the leaf veins or along the leaf edges, which expand and become confluent, finally resulting in chlorotic and necrotic stripes with only narrow green stripes along the midribs. In most cases, the affected leaves finally assume “tiger stripe” appearance. Symptoms on the grape berries include the appearance of small brown or purple spots particularly on table grapes (Surico *et al.*, 2008). Apoplexy, consisting of the partial or complete sudden wilting of the crowns, mainly occurring on GLSD, esca or esca proper-affected plants, is regarded as one of the symptoms or as the severe form of these diseases (Surico *et al.*, 2008; Letousey *et al.*, 2010; Bertsch *et al.*, 2013). Thus, affected plants die within a few years (Larignon *et al.*, 2009). To further understand the mechanisms of these decline-associated trunk diseases and their symptoms, several studies have been conducted on related grapevine responses. A perturbation of photosynthesis, accompanied by decreased gas exchange and photosystem II activity, has been reported in leaves of apoplectic and esca proper affected plants (Petit *et al.*, 2006; Letousey *et al.*, 2010; Magnin-Robert *et al.*, 2011). Disruption of photosynthesis may originate from damaged intracellular structures (Valtaud *et al.*, 2009). In the leaves of apoplectic grapevines, drastic physiological alterations of photosynthesis are coincident with decline in water use efficiency and activation of stress responses within at least 7 days preceding the appearance of visible symptoms (Letousey *et al.*, 2010). To obtain further information about the mechanisms activated in apoplectic and esca proper affected plants, Spag-

nolo *et al.* (2012) focused on the proteome variations of green stems. Their results indicated that similar responses are likely to be activated in asymptomatic stems, but various quantitative expression is triggered upon the onset of apoplexy or esca proper symptoms, while both kinds of plants are infected by the same pathogenic fungi. Leaves and green stems of *Vitis vinifera* L. plants affected by trunk diseases showed physiological and metabolic changes related to the external symptoms, although no pathogens associated with esca proper or other trunk diseases have been isolated from these organs (Magnin-Robert *et al.*, 2011; Spagnolo *et al.*, 2012). It was hypothesized that these external symptoms are caused by toxins produced by fungi in the woody tissues and then translocated to the leaves via the transpiration stream (Mugnai *et al.*, 1999). On the other hand, responses are still poorly described in woody tissues commonly infected by these pathogens.

This paper describes a two dimensional gel electrophoresis (2-DE)-based proteomic study of grapevine responses in woody tissues of apoplectic (A) and esca proper (E) affected vines. The main aims were to monitor global changes associated with wood symptoms and identify those proteins differentially expressed in the discolored or asymptomatic wood of apoplectic and esca proper affected plants. For 11 selected proteins identified by nanoLC-MS/MS, the expression of related genes was analysed by using qRT-PCR analysis.

Materials and methods

Plant material

Fifteen standing vines (cv. Chardonnay/ 41B) were uprooted in 2010 from a 26-year-old vineyard located in the Champagne-Ardenne region (France) owned by the company Moët & Chandon. Three plants per target external leaf symptom (GLSD or apoplexy) and three asymptomatic plants were collected. Asymptomatic plants were chosen from among those that had not shown either GLSD or apoplexy symptoms since 2001 and were thus regarded as visually unaffected plants (control plants, C). The trunks of all the collected plants were inspected internally for the presence of grapevine trunk disease fungi in asymptomatic or in discolored wood. Typical wood symptoms of GLSD and esca were recorded in all plants examined, including control plants. Plants showing foliar symptoms of GLSD were considered

as esca proper (E) affected plants. Two kinds of wood samples from trunks were selected for the proteomic and transcripts analysis: asymptomatic and black streaked trunk (BST) wood. Black streaking, which consists of single or more xylem vessels gathered into individual blackish brown bundles (Surico *et al.*, 2008) or scattered through whole trunk sections, was the most representative symptom observed in our sampling. Therefore, six groups of samples were defined for the study: asymptomatic trunk wood of control (C1), apoplectic (A1) as well as esca proper affected plants (E1); and black streaked trunk wood of control (C2), apoplectic (A2) and esca proper affected plants (E2) (sampling strategy outlined in supplementary Figure 1). Three biological replicates per group (i.e., three wood samples from three different plants) were taken. Woody tissues used for protein extraction and RNA extraction were frozen in the field with liquid nitrogen and subsequently stored at -80°C . Before each analysis, the required amount of biological sample was ground to a fine powder in liquid nitrogen with a Mixer Mill MM 400 (Retsch, Haan, Germany).

Isolation and identification of fungal pathogens

Trunks of the vines were inspected internally for the presence of discolorations associated with grapevine trunk diseases, and subsequently subjected to fungal isolation as described by Spagnolo *et al.* (2012). The fungal isolates obtained were identified according to the methods of Crous and Gams (2000) (for Pch), Essakhi *et al.* (2008) (for Pal), Fischer (2002) (for Fom), Phillips (2002) and Crous *et al.* (2006) (for Botryosphaeriaceae) and Carter (1994) (for *E. lata*).

Protein extraction

The total protein fraction from woody samples was isolated using a phenol-based procedure according to Spagnolo *et al.* (2012). The powdered tissue was placed in microtubes (0.30 ± 0.01 g of powder per 2 mL microtube) and then resuspended in 1 mL of cold acetone. After vortexing thoroughly for 30 s, the tubes were centrifuged at 10^4 g for 5 min at 4°C . The resultant pellet was washed once with cold acetone. The pellet was sequentially rinsed with cold 80% acetone three times or until the supernatant was colourless, then resuspended in 1 mL of cold 20% (w/v) trichloroacetic acid (TCA)/ H_2O . The suspen-

sion was sonicated in a water bath at 4°C for 10 min. After centrifugation, the pellets were sequentially washed twice with 20% (w/v) TCA/ H_2O and twice with 80% (v/v) acetone. This pellet was air-dried and the dry powder was resuspended in 0.7 mL dense sodium dodecyl sulphate (SDS) buffer [30% (w/v) sucrose, 2% (w/v) SDS, 0.1 M tris(hydroxymethyl) aminomethane (Tris)-HCl pH 8.0, 5% (v/v) 2-mercaptoethanol]. Then 0.8 mL of a 90% phenol water solution (Sigma-Aldrich) was added, and the resulting mixture was vortexed for 30 s. The phenol phase, recovered by centrifugation at 10^4 g for 5 min at room temperature, was separated in two aliquots. One of 0.7 mL was transferred to a 15 mL Falcon tube while an aliquot of 0.1 mL was placed in a 1.5 mL microtube. Further steps were followed in parallel. After addition of 5 volumes of cold 0.1 M ammonium acetate in methanol, proteins were precipitated from the phenol phase overnight at -20°C . The precipitated proteins were recovered by centrifugation, washed twice with cold 0.1 M ammonium acetate in methanol and twice with 80% (v/v) acetone. The final pellet was air-dried and stored at -80°C . The pellet retrieved from the aliquot of 0.1 mL was dissolved in 100 mL of 8 M urea for protein quantification using the Pierce 660 nm Protein Assay Kit (Thermo Fisher Scientific) and bovine serum albumin (BSA) as standard. After quantification, protein samples were solubilised in a sample buffer consisting of 7 M urea, 2 M thiourea, 4% (w/v) 3-[(3-cholamidopropyl)-dimethylammonio]-1-propanesulfonate (CHAPS), 0.5% (v/v) immobilized pH gradient (IPG) buffer 3-10, 60 mM 1,4-dithiothreitol (DTT), and traces of bromophenol blue.

Two-dimensional electrophoresis (2-DE)

For preparative 2-DE analysis, samples containing approximately 40 μg of total protein fraction were diluted in a mixture containing sample buffer and 10% (v/v) glycerol to a final volume of 125 μL . Immobilized pH gradient (IPG) gel strips (ReadyStrip IPG, pH 4–7, 7 cm, Bio-Rad, Hercules, CA, USA) were actively rehydrated during 15 h at 20°C with the mixture. Isoelectric focusing (IEF) was conducted at 20°C in an IPGphor unit (Amersham Pharmacia) as follows: a linear increase from 50 to 4000 V (during 2.5 h) to give a total of 10^4 V·h. Focused proteins were reduced and subsequently alkylated according to Görg *et al.* (1987). IPG strips were then placed on the top of vertical slabs of polyacrylamide (12% T and

2.6% C) and sealed by a layer of 1% (w/v) low melting point agarose, 0.15 M Bis-Tris/ 0.1 M HCl, and 0.2% (w/v) SDS. Electrophoretic migration along the second dimension was performed using a Mini-Protean 3 Cell (Bio-Rad) under a voltage of 30 V for 20 min, followed by 150 V for 1.5 h. After completion of SDS-polyacrylamide gel electrophoresis (PAGE), gels were stained with colloidal Coomassie Brilliant Blue using the PageBlue™ Protein Staining Solution (Fermentas) following the manufacturer's instructions.

Image analysis

Digitized images at 36.6 μm resolution were obtained using the GS-800 scanner and Quantity One 4.6.2 software (Bio-Rad). Computerized 2D gel analysis, including spot detection and quantification, was performed using the PDQuest Basic 8.0.1 software (Bio-Rad). The relative molecular mass was calibrated with internal protein markers (Precision Plus Protein Standards, Bio-Rad) after co-migration during the 2nd dimension. Quantification of detected protein spots was performed calculating the relative optical density \times area (relative OD \times area) in the gels. Normalization was set up according to the total spot density. Three biological repetitions per group were considered to detect qualitative and quantitative differences in protein expression among the six groups. The mean relative OD \times area \pm SD ($n = 3$) values of each group were used to estimate relative expression level (relative OD \times area %) of each protein spot among the groups. Differences among the means were evaluated by the Dunn's Multiple Comparison Test, after which the null hypothesis (equal means) was rejected in the Kruskal-Wallis test, assuming a significance of $P \leq 0.05$. The relative expression ratio to C1 in the other groups was also estimated. Values greater than 2 were considered positive response, or less than 0.5 as nil responses.

Protein identification by mass spectrometry

Protein spots of interest were excised manually and submitted to in-gel digestion. Reduction, alkylation and tryptic in-gel digestion were performed as previously described (Spagnolo *et al.*, 2012). Tryptic digests were analyzed by C18 reversed phase nanoHPLC on a nanoHPLC-Chip/MS system (Agilent Technologies) coupled to an ion trap amaZon

mass spectrometer (Bruker Daltonics). The complete system was controlled by Hystar 3.2 (Bruker Daltonics). For tandem MS experiments, the system was operated in the data-dependant mode with 6 MS/MS scans.

Mass data collected during nanoLC-MS/MS were processed, converted into ".mgf" files with DataAnalysis 4.0 (Bruker Daltonics) and interpreted using the MASCOT 2.3.02 algorithm (Matrix Science) and Open Mass Spectrometry Search Algorithm (OMSSA). Searches were performed without any molecular weight or isoelectric point restrictions against an in-house generated protein database composed of protein sequences of *Vitis*, human keratins and trypsin, downloaded from the National Center for Biotechnology Information nonredundant database (NCBIInr, June 19, 2012) concatenated with reversed copies of all sequences (total 138416 entries). Database searching was carried out using the following parameters: two missed cleavages; a parent and fragment mass tolerance of ± 0.25 Da; carbamidomethylation, N-terminal acetylation, and oxidized methionine as variable modifications.

Mascot and OMSSA results were loaded into the Scaffold 3.6.5 software (Proteome Software Inc.). To minimize false positive identifications, results were subjected to very stringent Mascot and OMSSA filtering criteria as follows: 1) for the identification of proteins, all peptides were validated with both algorithms (Mascot and OMSSA); 2) for proteins identified with two peptides or more, OMSSA $-\text{Log}$ (E-Value) scores were greater than 7, Mascot ion minus identity scores (the 95% Mascot significance threshold) greater than -5 and each ion scores were greater than 30; 3) in the case of single peptide hits, OMSSA $-\text{Log}$ (E-Value) scores were greater than 8, Mascot ion minus identity scores were greater than 10 and unique peptide ion scores greater than 30. The target-decoy database search allowed us to control and estimate the false positive identification rate of the study (Elias and Gygi, 2007). Thus, the final catalogue of proteins corresponded to an estimated false positive rate of less than 1%.

A list of all identified proteins with Mascot and OMSSA is provided in supplementary Table 1, and the spectra of single peptide hits is listed in supplementary Table 2. The MS data have been submitted to the PRIDE proteomics identification database (Vizcaíno *et al.*, 2010) (www.ebi.ac.uk/pride) under accession numbers # (27098).

Spot clustering and functional classification of identified proteins

Identified protein spots were classified according to the relative expression values (relative OD \times area %) in each group by performing hierarchical tree clustering with the NCSS 8 software by NCSS Statistical Analysis & Graphics (<http://www.ncss.com/>). Clustering parameters were set up as follows: group average (unweighted pair-group) linkage type, Euclidean distance method, average absolute deviation scaling method, cluster cutoff at 0.01.

A functional classification of the identified proteins was performed by using GenomeNet Database Resources (<http://www.genome.jp/kegg>) or according to their roles described in the literature.

Plant RNA extraction

Total RNA was isolated from three \times 50 mg of woody tissues powder using the plant RNA purification reagent (Invitrogen). The RNA pellet was re-suspended in 20 μ L of RNase free water, then treated with RQ1 DNase enzyme (Promega) and quantified by measuring the absorbance at 260 nm according to the manufacturer's instructions (Biowave DNA Spectrophotometer, Biochrom WPA).

Real-time RT-PCR analysis of gene expression

In total, 150 ng of total RNA were reverse-transcribed using the Verso SYBR 2-step QRT ROX enzyme (ABgene) according to the manufacturer's protocol. PCR conditions were as described by Bézier *et al.* (2002). Expression of 11 targeted genes selected from proteomic results was tracked by quantitative Reverse-Transcripts Polymerase Chain Reaction (qRT-PCR), including the α -chain elongation factor 1 gene (*EF1- α*), which was used as the internal standard to normalize the starting template of cDNA. This analysis was performed using the following gene-specific primers presented in supplementary Table 3. The cDNA sequence was obtained on NCBI Blast protein website (<http://blast.ncbi.nlm.nih.gov/>). We used the accession number (gi) of the targeted protein (*Vitis vinifera*) to search and obtain the corresponding cDNA sequence. Primers were designed at 60°C T_m to amplify fragments from 110 to 220 bp using Primer express 2.0 software (Applied Biosystems). The cDNA sequences were tested under NCBI Blast nucleotide to check their theoretical spe-

cific character to the targeted gene and not to a gene family. The amplification specificity of each qRT-PCR was confirmed by the presence of a single peak in the melt curve analysis, and no primer dimers were detected using agarose gel electrophoresis. Reactions were carried out in a real-time PCR detector Chromo 4 apparatus (Bio-Rad) using the following thermal profile: 15 s at 95°C (denaturation) and 1 min at 60°C (annealing/extension) for 40 cycles. The efficiency of the primer sets was estimated by performing real-time PCR on several dilutions. The results were normalized with the *EF1- α* gene and expressed relative to the control corresponding to asymptomatic- or BST-wood collected from control plants. PCR reactions were performed in duplicate for three biological replicates, for each of the six groups of samples. The results presented correspond to the means (\pm standard deviation) of the independent experiments.

Results

Isolation of fungal species associated with grapevine trunk diseases

The major causal agents of esca proper (Pch, Pal and Fom) were isolated from discolored woody tissues of the three groups of plants analyzed (E, A, and control plants). Fom was directly linked to white decay. Other fungi associated with grapevine trunk diseases, such as Botryosphaeriaceae species (Spagnolo *et al.*, 2011) and *Eutypa lata* (Kuntzmann *et al.*, 2010), were also isolated from woody tissues as shown in supplementary Table 4.

In contrast, no fungi were isolated from non-discoloured wood of the trunks and branches of control or diseased plants (supplementary Table 4).

Differences in protein yield and number of spots detected among the groups of samples

Protein yield was related to the type of wood samples, asymptomatic (C1, A1, E1) or BST (C2, A2, E2), but not to the absence/presence of external crown symptoms (wilted and tiger striped leaves). In fact, values of 0.31 ± 0.03 , 0.33 ± 0.04 and 0.27 ± 0.06 μ g mg⁻¹ of fresh weight were observed for C1, A1 and E1, respectively, whereas values of 0.11 ± 0.07 , 0.12 ± 0.08 and 0.10 ± 0.06 μ g mg⁻¹ of fresh weight were obtained in the case of C2, A2 and E2, respectively. The lower protein yield recorded from the BST wood samples

could be the result of altered physiology and/or the possible presence of phenolic compounds interfering with the protein extraction (Charmont *et al.*, 2005). On the other hand, the average number of protein spots resolved on 2-DE gels was not significantly different among the six groups in the pH range used in this study (pH 4–7). Indeed, means ranged between 148 ± 8 (A1) and 152 ± 6 (E2). This could indicate that the proteome variations occurring in the BST wood were mainly quantitative, as observed for the 27 differentially expressed protein spots selected for identification (supplementary Figure 2). The coefficients of variation associated with the number of spots detected in the biological replicates were 3.74% for C1 samples, 5.02% for C2, 5.11% for A1, 4.00% for A2, 3.70% for E1 and 4.01% for E2.

Identification of differentially expressed protein spots by nanoLC-MS/MS

A total of 148 protein spots were matched and compared by image analysis. Among the differentially expressed spots for at least one group, 27 were

subjected to in gel trypsin digestion followed by nanoLC-MS/MS analysis. In most cases, more than one protein was identified in each spot (supplementary Table 1), resulting in a large number of unique proteins to be analyzed. These 153 identified proteins were classified into nineteen functional groups using the GenomeNet Database Resources website (<http://www.genome.jp/kegg>) and other reports in the literature (Figure 1). Among the identified proteins, 12% were classified as being involved in the stress response, 10% in carbohydrate metabolism and in cellular processes, 8% in translation, 7% in transcription, 6% in protein destination and 5% in secondary metabolism (Figure 1). A selection based on their biological importance was performed, and a total of 53 proteins were chosen (Table 1). As shown in Table 1, experimental and theoretical molecular weights (Mw) correlated more closely than related isoelectric points (pI). Pearson's correlation coefficient ($P \leq 0.05$) was 0.920 for the Mw comparisons and 0.402 for the pI comparisons. The strongest discrepancies concerning the Mw were recorded in spots s3409, s6201, s6203 and s7319, where ratio values as high

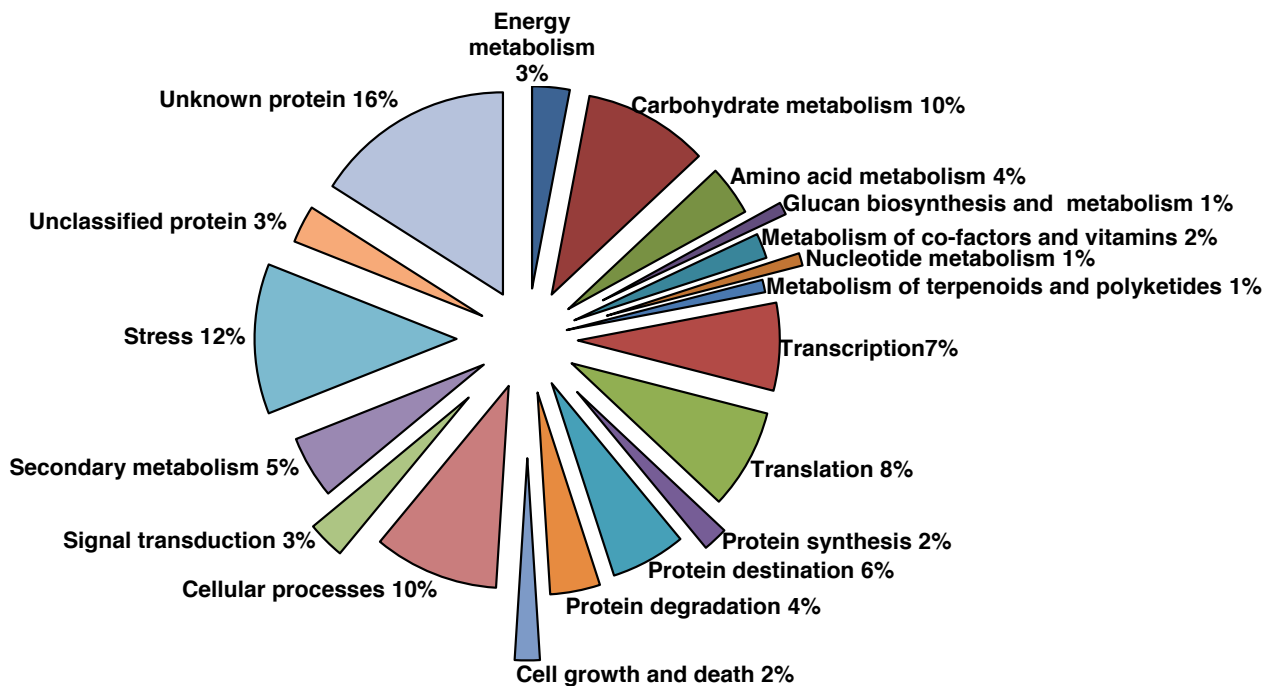


Figure 1. Functional classification of identified proteins from the trunks of fieldgrown *Vitis vinifera* plants affected or not by the grapevine trunk disease. The proteins were classified into 19 functional groups by using GenomeNet Database Resources website (<http://www.genome.jp/kegg>) and reports in the literature.

Table 1. Identified proteins differentially expressed in the black streaked or asymptomatic trunk wood of control, apoplectic and esca proper affected grapevines.

Spot ^a	Mw/p/ exp. ^b	Mw/p/ theor. ^c	Matched Protein ^d	Number of unique peptides ^e	Total number of peptides ^f	Coverage % ^g	Accession No. ^h
1007	11.00/4.40	18.98/4.84	PREDICTED: uncharacterized protein LOC100854560 [<i>Vitis vinifera</i>]	2	2	11	gi 359496362
1105	19.50/4.85	24.03/4.94	putative thaumatin-like protein [<i>Vitis hybrid cultivar</i>]	7	7	39	gi 7406716
1202	24.00/4.80	28.76/4.80	PREDICTED: 14-3-3-like protein [<i>Vitis vinifera</i>]	4	4	20	gi 359492927
1202	24.00/4.80	27.51/5.38	class IV endochitinase [<i>Vitis vinifera</i>]	1	1	6	gi 2306813
1208	29.50/4.18	31.54/6.59	PREDICTED: GEM-like protein 5 [<i>Vitis vinifera</i>]	1	1	4	gi 225468805
2211	22.50/5.12	20.90/4.83	PREDICTED: salt stress root protein RS1 isoform 3 [<i>Vitis vinifera</i>]	2	2	16	gi 225424944
2211	22.50/5.12	26.08/5.22	PREDICTED: endo-1,3;1,4-beta-D-glucanase [<i>Vitis vinifera</i>]	2	2	11	gi 225436938
2212	23.00/4.90	29.31/5.05	PREDICTED: acid phosphatase 1-like [<i>Vitis vinifera</i>]	3	3	17	gi 225445051
2212	23.00/4.90	24.03/4.80	PREDICTED: 14-3-3 protein 1-like [<i>Vitis vinifera</i>]	12	12	56	gi 359492927
2302	40.25/5.00	48.08/5.51	PREDICTED: transaldolase isoform 1 [<i>Vitis vinifera</i>]	10	10	30	gi 225425280
3105	18.75/5.30	25.01/6.35	PREDICTED: small heat shock protein, chloroplastic [<i>Vitis vinifera</i>]	6	6	24	gi 225455238
3107	18.12/5.45	25.01/6.35	PREDICTED: small heat shock protein, chloroplastic [<i>Vitis vinifera</i>]	5	5	24	gi 225455238
3202	17.50/4.90	25.01/6.35	PREDICTED: small heat shock protein, chloroplastic [<i>Vitis vinifera</i>]	10	10	45	gi 225455238
3203	17.19/5.05	25.01/6.35	PREDICTED: small heat shock protein, chloroplastic [<i>Vitis vinifera</i>]	8	8	43	gi 225455238
3409	45.12/5.40	49.65/4.95	PREDICTED: tubulin alpha-1 chain [<i>Vitis vinifera</i>]	15	15	47	gi 225435758
3409	45.12/5.40	52.45/5.51	PREDICTED: hexokinase-2, chloroplastic [<i>Vitis vinifera</i>]	15	15	40	gi 225457987
3409	45.12/5.40	54.45/5.71	PREDICTED: mitochondrial-processing peptidase subunit alpha [<i>Vitis vinifera</i>]	8	8	22	gi 225445041
4004	12.45/5.60	17.34/5.94	PREDICTED: 17.9 kDa class II heat shock protein [<i>Vitis vinifera</i>]	3	5	44	gi 225429604
4004	12.45/5.60	15.62/10.58	PREDICTED: 60S ribosomal protein L27-3 isoform 1 [<i>Vitis vinifera</i>]	1	1	8	gi 225423704
4102	12.60/5.36	21.71/5.87	PREDICTED: superoxide dismutase [Cu-Zn], chloroplastic [<i>Vitis vinifera</i>]	4	4	30	gi 225436450

(Continued)

Table 1. (Continued)

Spot ^a	Mw/p/ exp. ^b	Mw/p/ theor. ^c	Matched Protein ^d	Number of unique peptides ^e	Total number of peptides ^f	Coverage % ^g	Accession No. ^h
4102	12.60/5.36	17.09/5.96	pathogenesis-related protein 10 [<i>Vitis</i> hybrid cultivar]	2	2	18	gi 163914213
4212	31.75/5.78	33.82/5.50	TPA: isoflavone reductase-like protein 4 [<i>Vitis vinifera</i>]	10	15	45	gi 76559892
4216	22.55/5.59	25.06/5.26	Chalcone--flavonone isomerase 2 [<i>Vitis vinifera</i>]	7	7	39	gi 158514257
4216	22.55/5.59	24.51/5.48	PREDICTED: proteasome subunit alpha type-2-B [<i>Vitis vinifera</i>]	2	2	14	gi 225423722
4221	20.70/5.78	24.89/5.24	PREDICTED: glutathione S-transferase F9 [<i>Vitis vinifera</i>]	10	10	54	gi 225446791
4221	20.70/5.78	25.23/5.67	PREDICTED: stem-specific protein TSJT1 [<i>Vitis vinifera</i>]	7	7	48	gi 225432548
4221	20.70/5.78	25.31/5.85	hypothetical protein VITISV_038846 [<i>Vitis vinifera</i>]	6	6	35	gi 147784683
4221	20.70/5.78	24.90/5.31	PREDICTED: proteasome subunit beta type-6 [<i>Vitis vinifera</i>]	1	2	12	gi 225429850
5215	21.25/6.06	25.23/5.67	PREDICTED: stem-specific protein TSJT1 [<i>Vitis vinifera</i>]	7	7	47	gi 225432548
5215	21.25/6.06	24.89/5.24	PREDICTED: glutathione S-transferase F9 [<i>Vitis vinifera</i>]	10	10	51	gi 225446791
5316	31.75/5.97	33.82/5.50	TPA: isoflavone reductase-like protein 4 [<i>Vitis vinifera</i>]	10	14	45	gi 76559892
5316	31.75/5.97	29.22/5.74	PREDICTED: dihydrofolate reductase [<i>Vitis vinifera</i>]	3	3	14	gi 225440230
5422	41.87/6.11	39.17/5.39	PREDICTED: peroxidase 12-like [<i>Vitis vinifera</i>]	10	10	36	gi 359493149
5422	41.87/6.11	43.56/5.63	PREDICTED: bifunctional polymyxin resistance protein ArnA [<i>Vitis vinifera</i>]	3	3	11	gi 225436371
5422	41.87/6.11	44.75/10.42	PREDICTED: 60S ribosomal protein L4 [<i>Vitis vinifera</i>]	6	6	21	gi 225439761
5422	41.87/6.11	42.91/5.49	S-adenosylmethionine synthase 4	2	2	6	gi 223635287
6001	11.87/6.08	17.34/5.94	PREDICTED: 17.9 kDa class II heat shock protein [<i>Vitis vinifera</i>]	5	7	60	gi 225429604
6001	11.87/6.08	21.82/9.20	PREDICTED: nitrogen regulatory protein P-II homolog [<i>Vitis vinifera</i>]	4	4	24	gi 225437667
6002	10.65/6.10	16.31/6.32	PREDICTED: glycine-rich RNA-binding protein GRP1A-like [<i>Vitis vinifera</i>]	7	7	57	gi 359475330
6002	10.65/6.10	15.26/5.49	PREDICTED: superoxide dismutase [Cu-Zn] isoform 2 [<i>Vitis vinifera</i>]	3	3	30	gi 225451120
6101	13.12/6.00	17.34/5.94	PREDICTED: 17.9 kDa class II heat shock protein [<i>Vitis vinifera</i>]	1	2	20	gi 225429604

(Continued)

Table 1. (Continued)

Spot ^a	Mw/pI exp. ^b	Mw/pI theor. ^c	Matched Protein ^d	Number of unique peptides ^e	Total number of peptides ^f	Coverage % ^g	Accession No. ^h
6101	13.12/6.00	17.09/5.96	pathogenesis-related protein 10 [<i>Vitis</i> hybrid cultivar]	3	3	25	gi 163914213
6203	19.37/6.16	21.72/5.81	PREDICTED: flavoprotein wrbA-like [<i>Vitis vinifera</i>]	5	5	31	gi 359496220
6203	19.37/6.16	17.09/5.96	pathogenesis-related protein 10 [<i>Vitis</i> hybrid cultivar]	2	2	18	gi 163914213
6203	19.37/6.16	31.52/7.71	PREDICTED: ATP-dependent Clp protease proteolytic subunit 5, chloroplastic isoform 1 [<i>Vitis vinifera</i>]	4	4	12	gi 225437581
6420	42.69/6.22	43.11/5.65	S-adenosylmethionine synthase 2 [<i>Vitis vinifera</i>]	10	10	43	gi 223635284
6420	42.69/6.22	51.31/6.61	PREDICTED: probable ornithine aminotransferase [<i>Vitis vinifera</i>]	12	12	36	gi 225443914
6420	42.69/6.22	46.43/5.80	PREDICTED: eukaryotic initiation factor 4A-3-like [<i>Vitis vinifera</i>]	9	9	25	gi 225464928
6420	42.69/6.22	46.27/5.99	PREDICTED: isocitrate dehydrogenase [NADP] [<i>Vitis vinifera</i>]	2	2	7	gi 225466253
6420	42.69/6.22	40.17/5.54	leucoanthocyanidin dioxygenase [<i>Vitis amurensis</i>]	2	2	8	gi 224038270
7210	20.60/6.57	24.61/6.88	PREDICTED: proteasome subunit beta type-1 [<i>Vitis vinifera</i>]	5	5	38	gi 225453909
7210	20.60/6.57	24.94/5.78	PREDICTED: glutathione S-transferase F9 [<i>Vitis vinifera</i>]	8	9	42	gi 225446793
7319	31.37/6.32	33.87/5.76	TPA: isoflavone reductase-like protein 5 [<i>Vitis vinifera</i>]	14	14	54	gi 76559894
7319	31.37/6.32	17.18/5.62	PREDICTED: MLP-like protein 28 [<i>Vitis vinifera</i>]	2	2	22	gi 225424272
7319	31.37/6.32	34.28/5.49	PREDICTED: glyoxylate reductase isoform 1 [<i>Vitis vinifera</i>]	2	2	12	gi 359482924
7319	31.37/6.32	35.04/6.05	PREDICTED: isoflavone reductase homolog [<i>Vitis vinifera</i>]	1	1	4	gi 359491809
7319	31.37/6.32	34.46/9.00	PREDICTED: 60S ribosomal protein L5-like isoform 2 [<i>Vitis vinifera</i>]	2	2	6	gi 225434146
7319	31.37/6.32	30.02/9.31	PREDICTED: 60S ribosomal protein L5-like [<i>Vitis vinifera</i>]	1	2	11	gi 359495418

^a Spot code as reported in Figures 3, 4 and S2.

^b Deduced spot molecular mass (kDa) and isoelectric point as observed on the gels.

^c Theoretical molecular mass (kDa) and isoelectric point computed using the compute Mw/pI tool in ExPASy Bioinformatics Resource Portal.

^d Protein identified via the MASCOT and OMSSA search engines against in house made database from NCBI database.

^e Number of unique peptides matching the protein sequence.

^f Total number of peptides matching the protein sequence.

^g Percentage of the protein sequence covered by the matching peptides.

^h Accession No. of the matched protein as reported in the NCBI database.

as 2 were found. In the case of the pI comparison, for some identified proteins the theoretical pI was found to be greater than 7 (spots s4004, s5422, s6001, s6201, s6203, s7319 and s8102). Such differences, as well as the presence of the same protein in several spots, may be due to the presence of protein variants and/or post-translational modifications, truncation or degradation products (Spagnolo *et al.*, 2012). The discrepancies between experimental and theoretical Mw values could also be due to the fact that some protein sequences contained a signal peptide in the database, which effectively increases the theoretical molecular mass since the whole sequences are considered for the calculation

Differentially expressed proteins among the groups of samples

Comparison of the relative expression values of the spots from the six groups showed that C2 had a similar protein expression to the other groups the largest number of times (71), whereas the lowest fre-

quency was observed for E1 (52) (Figure 2a). When all the possible pairs were considered separately, the most similar protein expression was recorded for the pairs A2-E2 (18 spots) and C1-A1 (16 spots), whereas the least similar was observed for C1-E1 and E1-E2 (nine spots) (Figure 2b). Although to a lesser extent than for the A2-E2 pair, a weak similar expression to A2 and E2 was also observed when the C2 group was considered (15 and 13 spots, respectively) (Figure 2b). However, taken together C2, A2 and E2 had similar expressions in only six spots (s1208, s2211, s2302, s3105, s3409, s4102) (Figure 2b). In this regard, it is important to note that the percentage of GLSD agent isolation was similar for C2, A2 and E2 (50–70% of the positive samples), but different frequencies of positive samples (where at least one fungal colony was detected) of 86% for E2, 50% for A2 and 41% for C2. Large differences in protein expression were apparent among the groups from asymptomatic wood (C1, A1 and E1). Except for the C1-A1 pair, the number of spots with similar protein expression became less when the E1 group was considered (Figure 2b). When the three

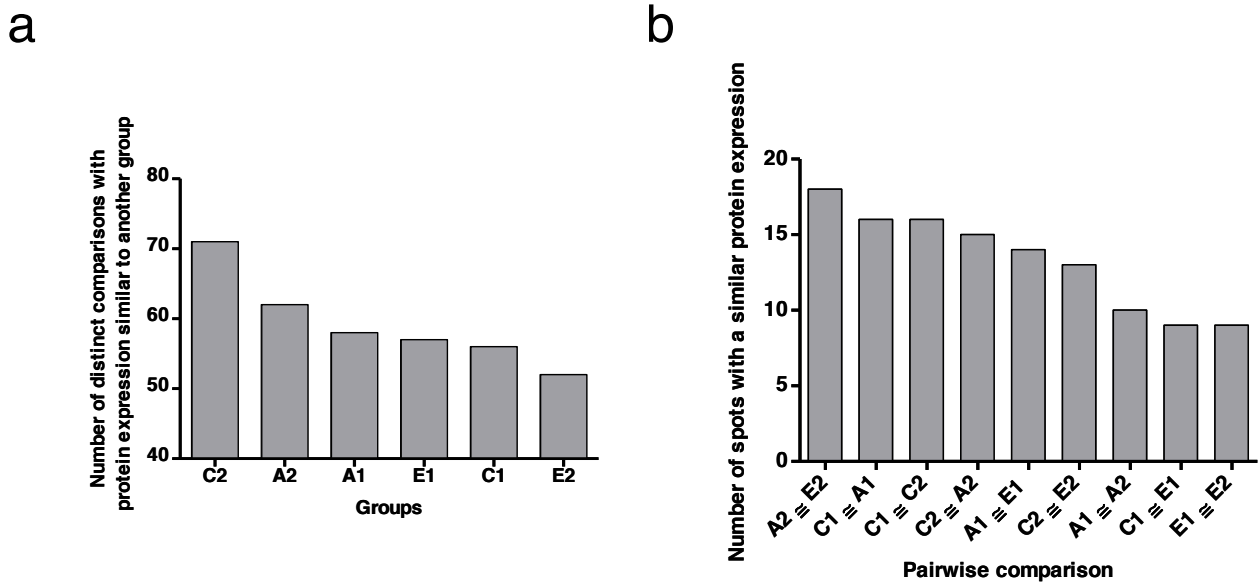


Figure 2. Pairwise comparisons of protein spots. **a**, Pairwise comparison for all the possible pairs of group samples in one spot performed for all the spots (135 total comparisons per group). The number of times where the relative expression value of each group was considered to be similar to another (ratio ≤ |2|) is reported. Asymptomatic (C1, A1, E1) and black streaked (C2, A2, E2) trunk wood of control (C1, C2), apoplectic (A1, A2) and esca proper affected (E1, E2) plants. **b**, Pairwise comparison involving samples from asymptomatic (C1, A1, E1) and black streaked (C2, A2, E2) trunk wood performed for all the spots (27 total comparisons per group). The number of times (spots) where their relative expression was considered to be similar (ratio ≤ |2|) is reported.

groups were considered together, they showed similar expression values only in three spots (s6203, s6420, s7319). Proteome variations were induced in the asymptomatic wood of apoplectic (A1) and esca proper affected (E1) plants. Moreover, differences in protein expression between asymptomatic and BST wood did not show the same trend among the groups of plants (C1-C2, A1-A2, E1-E2), being more marked in A and E affected plants. The most similar protein expression was registered for the C1-C2 pair (16), followed by A1-A2 (10) and E1-E2 (9) (Figure 2b).

Proteomic changes in asymptomatic and BST wood

To obtain a comprehensive overview of the dynamics of protein abundance associated with foliar symptom development, hierarchical tree clustering was performed and protein abundance patterns were grouped together without *a priori* knowledge of the biological reasons for the existence of these groups (Figure 3). Moreover, proteins were described and discussed according to their putative biological functions (Figure 1).

The hierarchical tree clustering analysis of the five spots (s2212, s2302, s3409, s6420) of carbohydrate metabolism (including glycolysis metabolism) indicated that the distribution of these spots was different between asymptomatic and BST wood, regardless of the external symptoms. During foliar symptom development, transaldolase (s2302), acid phosphatase 1-like (s2212), hexokinase 2 (s3409), isocitrate dehydrogenase (s6420) appeared to be all down-accumulated in asymptomatic wood of diseased plants, irrespective of the external symptoms (A or E). Conversely, the transaldolase (s2302) was more abundant in A2 and E2 as compared to C2 (Table 1, Figure 4). In parallel to the proteomic analysis, we followed the *transaldolase* gene expression, which did not correlate with the protein level (Figure 5). No predictions of protein levels present in the organ could be formulated with transcript analysis.

Plant growth was especially perturbed. A GEM-like protein 5 (s1208) implicated in tissue growth was identified. Protein levels in A1 and E1 were lower than those observed in C1. Additionally, an endo-(1,3)-(1,4)- β -D-glucanase (s2211) associated with modulation of cell growth showed less abundance in wood of diseased plants A1 and E1 (Table 1, Figure 4). Dihydrofolate reductase (DHFR, s5316), a small enzyme that plays a supporting but essen-

tial role in the building of DNA during cell division, appeared to be down-regulated during symptom development. Alteration of cell wall biogenesis was also observed and concerned the production of the cell wall sugar D-apiose. The polymyxin resistance protein ARNa (s5422) has 97% homology to an UDP-apiose/UDP-xylose synthase.

Nitrogen metabolism was also altered with the appearance of foliar symptoms, through the perturbation of an ornithine aminotransferase (s6420) amount. Moreover, a nitrogen regulatory protein II (PII, s6001), a nuclear-encoded plastid protein that regulates ornithine and arginine biosynthesis, was less abundant in A1 and E1 in comparison to C1.

The distribution of the eight spots containing proteins involved in protein synthesis and degradation (s3409, s4004, s4216, s4221, s5422, s6203, s7210, s7319) (Table 1, Figure 3) was different in control plants depending on the sample state, C1 and C2 (Figure 3). Abundance of seven of these spots (s4004, s4216, s4221, s5422, s6203, s7210, s7319) was altered in the trunks of grapevines affected by apoplexy (Figure 3). Instead, the relative abundance of six spots (s4004, s4216, s4221, s5422, s7210, s7319) was affected during GLSD appearance (Figure 3). The impact of foliar symptom development on proteins variations varied depending on the type of sample. For instance, proteasome subunit beta (s7210) was down-regulated in asymptomatic wood (A1, E1) and up-regulated in BST wood (A2, E2).

Two small heat shock proteins (smHSPs) were identified: a smHSP chloroplastic (smHSPCP, s3105-s3107-s3202-s3203) and a 17.9 kDa class II HSP (HSP17.9; s4004-s6001-s6101) (Table 1). Hierarchical tree clustering also indicated that, in these cases, the distribution of the corresponding spots depended on the sample state, asymptomatic or BST wood (Figure 3). These spots were mainly grouped in the clusters (1, 2 or 3) with the greatest abundance in C1, E1 and A1. They were also grouped in clusters (2 or 3) with less abundance in wood with the presence of fungi. The two smHSPs (s3105-s3107-s3202-s3203 and s4004-s6001-s6101) showed less abundance in A1 and E1 in comparison to C1. Results of transcript analysis for *smHSPCP* corroborated the results of protein expression (Figure 5). Hierarchical tree clustering indicated that the distribution of the spots (s4221, s5215, s6002, s7210), containing proteins involved in antioxidant system, was independent of the sample state in control plants (Figure 3). The abundance of

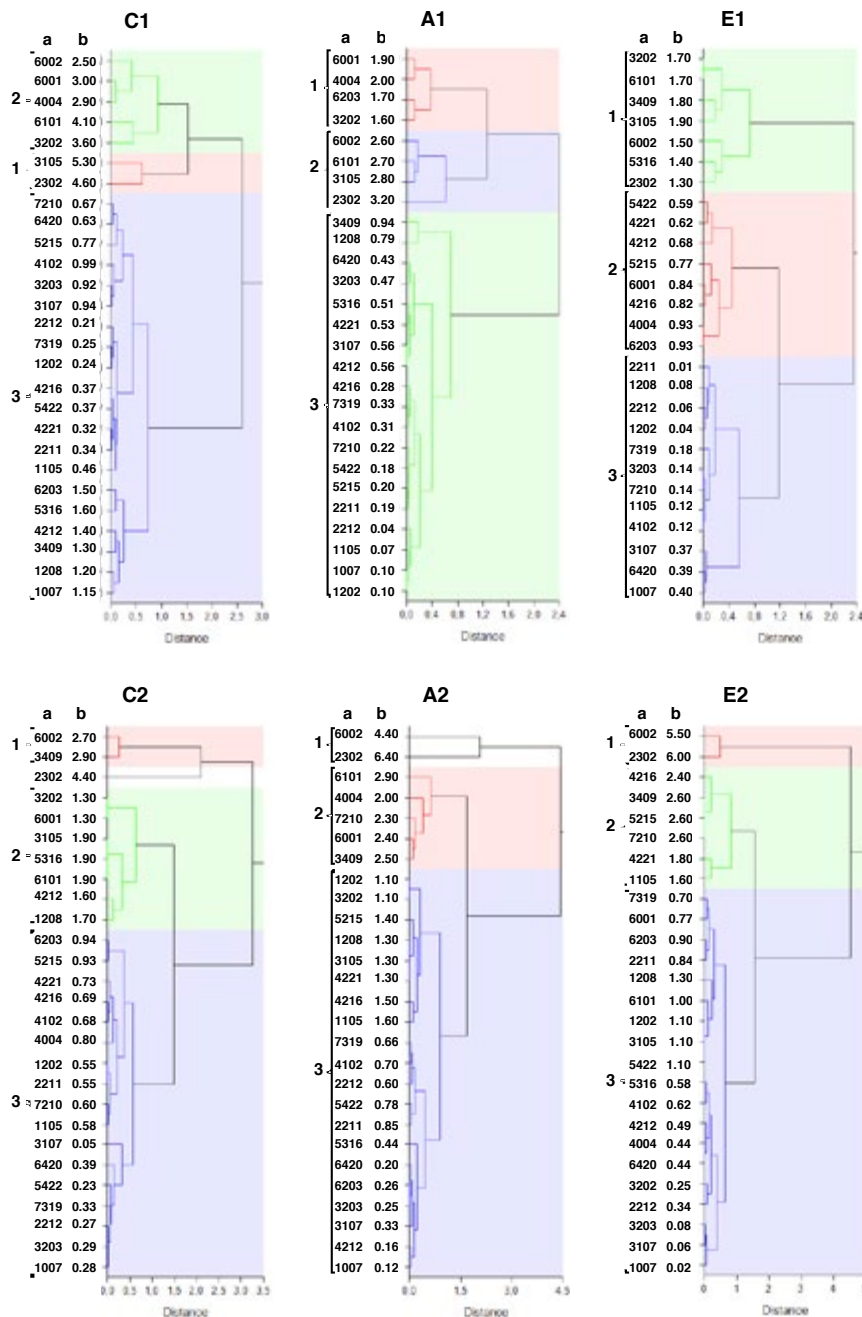


Figure 3. Hierarchical tree clustering based on relative expression values of the 27 differentially expressed protein spots identified in the groups of asymptomatic (C1, A1, E1) and black streaked wood (C2, A2, E2) from control (C1, C2), apoplectic (A1, A2) and esca proper affected grapevines (E1, E2). The relative value of optical density \times area (relative OD \times area %) of the total value observed in the gel images was considered as a measure of expression. Relative mean values are from three relative values obtained by dividing the value of each spot to the total density of the corresponding gel. Hierarchical tree clustering was performed using the NCSS 8 software by NCSS Statistical Analysis & Graphics (<http://www.ncss.com/>). Clustering parameters were set up as follows: group average (unweighted pair-group) linkage type, Euclidean distance method, average absolute deviation scaling method, cluster cutoff at 1.0. Numbers in parentheses indicate clusters from greatest values (cluster 1) to the smallest (cluster 3). Column a: spot number; column b: relative expression value.

these spots was affected during foliar symptom development depending on the proteins and external symptoms (Figures 2 and 3). The two isoforms of glutathion S-transferase (GST) F9 (s4221-s5215 and s7210) and the superoxide dismutase chloroplastic (SODCP) (s4102) were less abundant in A1 and E1, whereas GSTF9s (s4221-s5215 and s7210) and SOD isoform II (s6002) were more abundant in A2 and E2 (Figure 3), in comparison to C1 and C2, respectively. No significant down- or up-regulation was observed for the related *GSTF9* or *SODCP* genes (Figure 5).

Regarding the defense response, a hypothetical protein (VITISV_038846) homolog to the “pathogen-

esis-related” protein (PR) PR-17 (s4221) was identified (Table 1). The transcript analysis suggested weak up-regulation of *PR-17* expression in E1 (Figure 5). Endochitinase (s1202) and thaumatin-like protein (TLP, s1105) showed decreased abundance in A1 and E1 and increased abundance in A2 and E2. *TLP* expression was significantly induced in A2 (80-fold) and E2 (26-fold) in comparison to C2 (Figure 5), and correlated positively with the protein abundance in BST wood of diseased grapevine. Spots containing PR10 (s4102-s6101) were less abundant in A1 and E1. Protein and transcript expressions of PR-10 were not significantly different between BST samples.

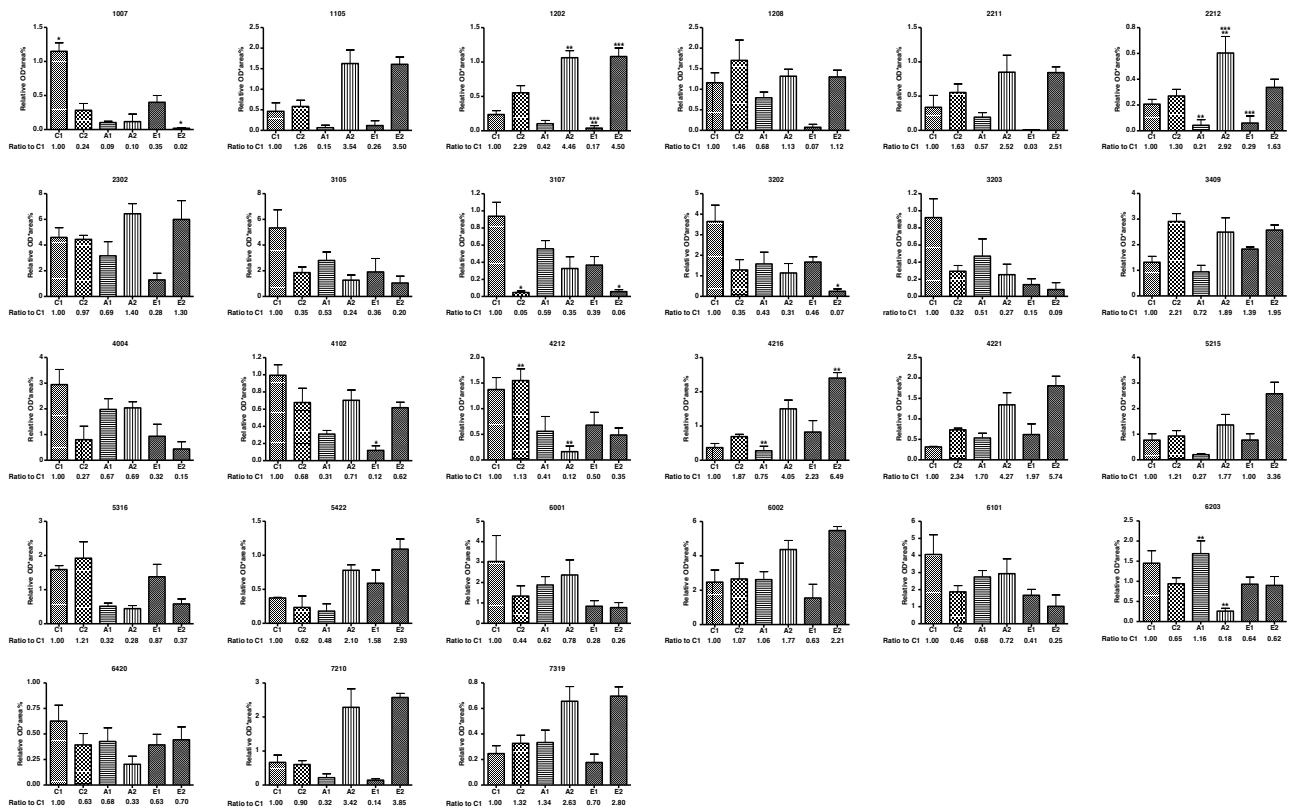


Figure 4. Quantification of differentially expressed proteins extracted from asymptomatic (C1, A1, E1) and black streaked (C2, A2, E2) trunk wood of control (C1, C2), apoplectic (A1, A2) and esca proper affected (E1, E2) grapevines. Vertical axis represents the relative value of optical density × area (relative OD × area %) of the total value observed in the gel images as a measure of expression. Histograms indicate the mean quantitative values (± standard deviation: SD) of three independent experiments. Relative mean values (± SD) are from three relative values obtained by dividing the value of each spot to the total density of the corresponding gel. Differences among the means were evaluated by the Dunn’s Multiple Comparison Test, and after that the null hypothesis (equal means) was rejected in the Kruskal-Wallis test, assuming a significance of $P \leq 0.05$. One asterisk indicates a statistically significant difference with the control C1. Two or three asterisks indicate statistically significant differences between the two classes where they were added. The relative expression ratio to C1 in the other groups is reported.

Secondary metabolism-related proteins identified in this study were involved in the phenylpropanoids pathway. Three sub-groups of proteins that changed in abundance with foliar symptom development were distinguished. The first comprised a single protein with increased abundance in both asymptomatic and BST wood (s4216, chalcone flavonone isomerase 2). The second also included a single protein with increased abundance in BST wood alone (s7319, isoflavone reductase homolog). The third sub-group included two proteins with decreased abundance both

in asymptomatic and BST wood (s4212-s5316, isoflavone reductase-like (IFRL) protein 4; s6420, leucoanthocyanidin dioxygenase) (Figure 4). Results of the supplementary analysis of transcripts highlighted the up-regulation of *CHI* in asymptomatic wood and the down-regulation of *IFRL4* (Figure 5). S-adenosyl-L methionine (SAM) synthase plays an important role in the production of SAM leading to polyphenols. Hierarchical tree clustering indicated that the distribution of the two forms of SAM (s6420 and s5422) varied depending on the sample observed;

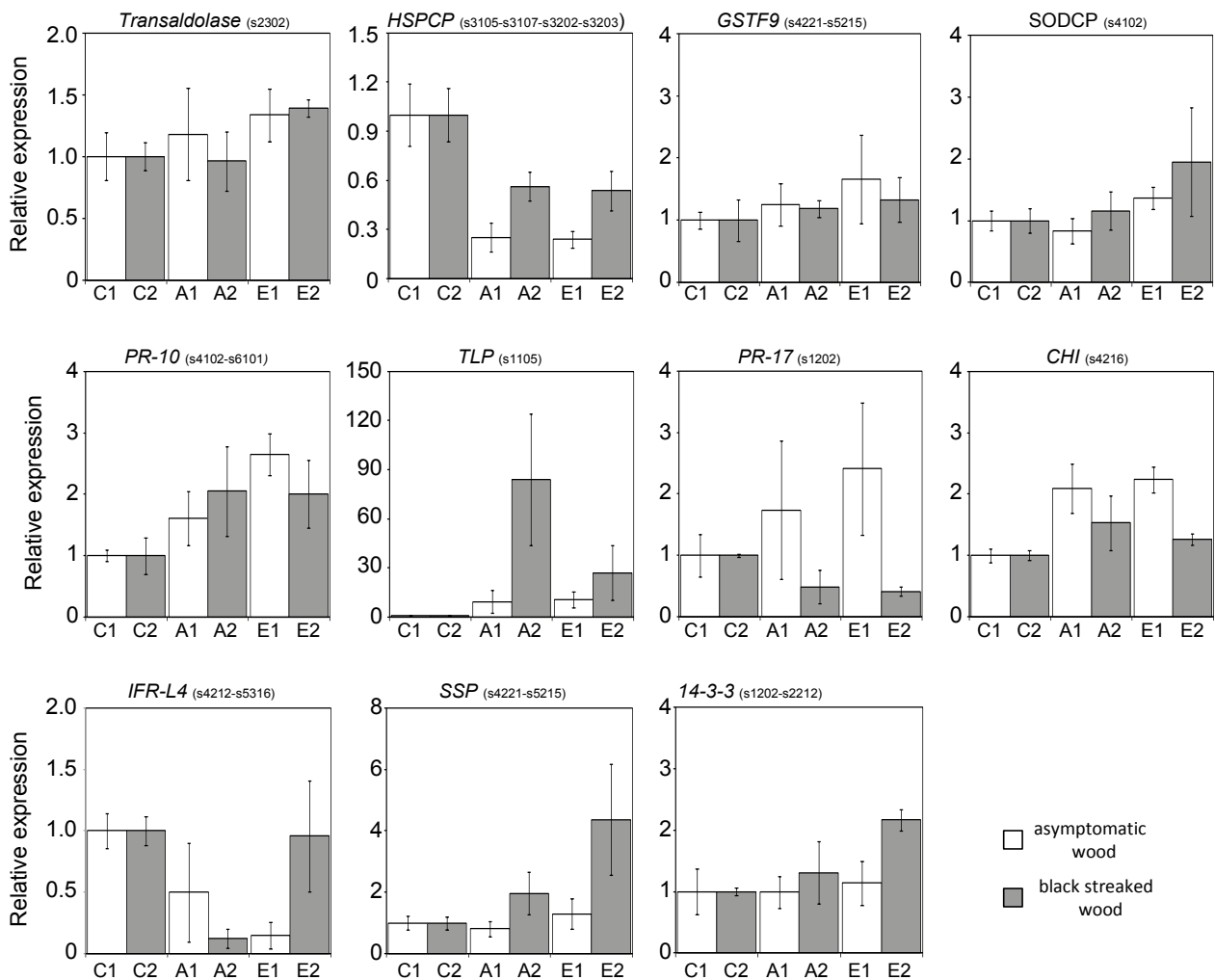


Figure 5. Expression levels of eleven selected genes in asymptomatic (C1, A1 and E1) and black streaked trunk wood (C2, A2 and E2) of control (C), apoplectic (A) and esca proper affected (E) 26 year-old standing grapevines (cv. Chardonnay) by quantitative reverse-transcription polymerase chain reaction. Results correspond to means (\pm standard deviation) of three independent experiences (C1, C2, A1, A2, E1 and E2). Gene expression was considered as significantly up- or down-regulated to the $1\times$ controls, when changes in relative expression were $> 2\times$ or $< 0.5\times$, respectively.

the two spots were grouped in the same cluster for E1 and C2 but not for C1, A1, A2 and E2 (Figure 3). These results may indicate a perturbation of these two proteins levels according to the external symptoms. The exact role of the six stress-induced proteins in plant defense is unclear. These six proteins showed decreased abundance in asymptomatic wood of diseased plants. They were identified as an uncharacterized protein (s1007) belonging to the PLAT family (polycystin-1 lipoxigenase alpha toxin domain), a stem specific protein TSJT1 (SSP, s4221-s5215), a glycine RNA binding protein (GR-RBP, s6002), a salt stress root protein RS1 isoform 3 (RS1; s2211); a 14-3-3 protein 1-like (14-3-3, s1202-s2212) and a major latex protein (MLP) like protein 28 (s7319) (Table 1). No correlation was observed between the transcript analysis and the proteins expression of both 14-3-3 and SSP (Figures 4 and 5). Nevertheless, four of them were accumulated in E2 and A2: 14-3-3 (s1202-s2212), GR-RBP (s6002), RS1 (s2211), and SSP (s4221-s5215) (Figure 4). Moreover, transcript analysis of SSP and 14-3-3 indicated significant up-regulation in E2 compared to A2 and C2 (Figure 5). These results revealed that protein and transcript expression during foliar symptom development varies according to the type of sample (asymptomatic or BST wood).

Discussion

Primary metabolism altered in the trunks of apoplectic and esca proper affected grapevines

Primary metabolism was altered. Several proteins involved in metabolic pathways (glucogenesis, citrate and pyruvate metabolism) were less abundant in diseased plants (transaldolase - s2302, acid phosphatase 1-like - s2212; hexokinase 2 - s3409, isocitrate dehydrogenase - s6420), and particularly in asymptomatic tissues (A1, E1). Moreover, as a consequence of the repression of primary metabolism, a negative effect on cell growth/division was also observed, e.g., diminution of the relative abundance of DHFR (s5316) and endo-(1,3)- β -glucanase (s2211). DHFR genes were up-regulated during the transition from primary to secondary growth (Ko *et al.*, 2004), and alteration of this protein accumulation may stop the growth or the division of living cells in wood and particularly the secondary growth (secondary vascular tissue formation). Alteration of nitrogen metabolism and especially the proline pathway was also observed. PII (s6001), a nuclear protein that regulates

a key enzyme in ornithine and arginine biosynthesis and the ornithine aminotransferase (OAT, s6420) involved in the ultimate formation of proline to ornithine, showed a decrease in the relative abundance in diseased grapevine (A, E). The inhibition of these pathways by the host plant may limit colonization of the trunk by the causal agents since certain amino acids (e.g., proline, asparagine, alanine) are well known to stimulate hyphal growth in fungi (Bélanger *et al.*, 1990). Thus, many studies have implicated proline metabolism in the plant-pathogen interaction (Deuschle *et al.*, 2004; Mitchell *et al.*, 2006). Associated with nitrogen metabolism modulation, proteins involved in protein synthesis and degradation, various 60SRP (s4004, s5422, s7319) proteins and subunits of the proteasome complex (s3409, s4216, s4221, s6203, s7210) were identified associated with GLSD and/or apoplexy symptom development. The activation of proteolysis observed in BST wood of both apoplectic and GLSD plants might increase disease development, as described in grapevine in response to *Phytoplasma* infection (Margaria and Palmano, 2011). Moreover, the over-regulation of ribosomal proteins indicates a positive role in aggravating pathogenesis by altering translation (Golkari *et al.*, 2007).

Carbohydrates act as metabolic signals that induce both the expression of defense-related genes and the repression of primary metabolism (Herbers *et al.*, 1996; Ehness *et al.*, 1997; Berger *et al.*, 2004). For example, the accumulation of soluble hexoses can regulate programmed cell death in plants (Kim *et al.*, 2006), suggesting that sugar sensing mediates a direct link between carbohydrate metabolism and the defense response. In this sense, proteasome activity has also been linked with activation of defense reactions (Suty *et al.*, 2003). Pathogen recognition by plants results in significant reprogramming of plant cells to activate and deploy defense responses to halt pathogen growth.

The majority of proteins identified in the trunks of apoplectic and esca proper affected grapevines related to cell rescue and defense

Small heat shock proteins

Small heat shock proteins (smHSPs, s3105-s3107-s3202-s3203 and s4004-s6001-s6101) play important chaperone roles in maintaining cellular functions when plants are subject to a variety of stresses. Because of their well-known role as chaperones, HSPs

were included in the protein destination category. However, many studies have suggested they are initially involved in heat stress, and later in various biotic or abiotic stresses (Al-Whaibi, 2011). Consistent with our data, a decrease in abundance of smHSPs in asymptomatic wood was observed in diseased plants, and could be related to the development of foliar symptoms. A similar down-regulated expression of one smHSP chloroplastic gene was observed in the leaves of a susceptible cultivar (Riesling) during *Plasmopara viticola* infection (Polesani *et al.*, 2008). Yang *et al.* (2011) reported that smHSPs were differentially expressed in Pierce's Disease (PD)-resistant and PD-susceptible genotypes in grapevine and might be implicated in tolerance. smHSPs could therefore be systemically induced in grapevines and may play a role in disease tolerance. Since an important key regulator of smHSPs is H₂O₂, the synthesis of smHSPs can be considered as an adaptive mechanism in which cellular protection against oxidative stress is essential (Banzet *et al.*, 1998; Vanderauwera *et al.*, 2005).

Antioxidant defense system

In this study, the expression of four proteins involved in the antioxidant system was also altered compared to control plants: one protein (SODCP, s4102) decreased in abundance, one (SODII, s6002) increased, and the other two one a decrease/increase (two isoforms of GSTF9, s4221-s5215 and s7210) in asymptomatic/BST wood of diseased plants, respectively. Reduced expression of SOD and GST was also reported in other organs of grapevine affected by trunk diseases, both leaves (Valtaud *et al.*, 2009; Camps *et al.*, 2010; Letousey *et al.*, 2010; Magnin-Robert *et al.*, 2011) and green stems (Spagnolo *et al.*, 2012). In spite of the over-regulation of antioxidant enzymes observed in BST wood, the grapevines show external symptoms (apoplexy or GLSD). These results suggest that the GST system is not related to host tolerance against pathogenic fungi, as emphasized by Valtaud *et al.* (2009). To prevent oxidative damage, GSTs perform diverse catalytic and non-catalytic roles in the detoxification of xenobiotics, such as toxins (Frova, 2003). The toxin eutypin, produced by another grapevine trunk disease agent, *Eutypa lata*, is metabolically active in the aldehyde form (Guillen *et al.*, 1998). The major wood-infesting fungi Pch, Pal and Fom have been shown to produce diverse toxins (Andolfi *et al.*, 2011). Toxins may un-

dergo similar processing leading to their detoxification in BST wood.

Defense responses

A PR-10 protein (s4102-s6101), an endochitinase (s1202), a TLP (s1105) and a homolog to a PR-17 (s4221) protein were identified, and changed in abundance, according to the external symptoms and type of wood. In the present study, the lower abundance of PR-10 in asymptomatic wood of diseased plants (A1, E1) may indicate that it plays a defensive role in the grapevine response to trunk disease fungal agents. This is supported by the increase of PR-10 expression noted in grapevine cell cultures in response to elicitors produced by Pch (Lima *et al.*, 2012). The class IV endochitinase, known to be induced in grapevine by pathogen infection (Camps *et al.*, 2010), is involved in plant defense through the hydrolysis of chitin fragments of fungal cell walls. Abundance of PR-10 changed, decreasing in asymptomatic wood and increasing in BST wood of diseased vines. Similar trends of protein expression were observed for TLP. These results were surprising because TLPs are normally expressed at low levels in healthy plants and rapidly accumulate to high levels in response to biotic stress (Fung *et al.*, 2008; Camps *et al.*, 2010). The thaumatin-like proteins belong to the PR-5 family (Afroz *et al.*, 2001), family members which have antifungal properties (Monteiro *et al.*, 2003). Considering both the expression levels of endochitinase and TLP, it is obvious that their changes in trunk tissues (decrease in asymptomatic wood or increase in BST wood) has no preventive effects on the onset of external symptoms. Finally, a hypothetical protein homolog to PR-17 was up-regulated in the trunks of diseased vines, but this induction does not avoid foliar symptom appearance. Transcript analysis of a PR-17 gene (called *NtPR27-like*) was similarly induced in grapevine leaves in response to *E. lata* infection (Camps *et al.*, 2010). Many plant defense responses involve the production of secondary metabolites (La Camera *et al.*, 2004). S-adenosyl-L methionine (SAM) synthase(s) participates in the production of SAM, leading to phenolic compounds involved in defense responses (Roje, 2006). Our study identified two SAMs (s5422 and s6420) with opposite evolution in trunk samples from vines during the development of foliar symptoms. The lowest level of SAMs occurred in symptomatic green stems of A and E affected plants (Spagnolo *et al.*, 2012). A

role for SAMs in the intrinsic resistance capability was suggested (Figueiredo *et al.*, 2008) correlated to up-regulation of transcripts in the *E. necator*- and *P. viticola*-resistant cultivar (Regent). Functions of phenylpropanoid compounds in plant defense range from preformed or inducible physical and chemical barriers against infection to signal molecules involved in local and systemic signaling for defense gene induction (Dixon *et al.*, 2002). With regard to the phenylpropanoid pathway, a chalcone flavanone isomerase (CHI) (s4216) was identified, which was more abundant in the trunks of diseased vines and especially in BST wood. In addition, two isoforms of isoflavone reductase (IFR, involved in biosynthesis of isoflavonoid phytoalexins, s7319 and s4212-s5316) and one leucoanthocyanidin dioxygenase (LDOX, involved in the anthocyanins biosynthesis, s6420) were identified, and these decreased in relative abundance in the asymptomatic wood of diseased vines. Hence, this alteration of the isoflavonoid/anthocyanin pathways may be related to the presence of external symptoms and/or to their possible imminent development. Similarly, Camps *et al.* (2010) associated the induction of *LDOX* gene expression to the lack of leaf symptoms on grapevine affected by *E. lata*. Thus, production of phenylpropanoid compounds was probably stimulated in BST wood of either apoplectic or esca proper affected vines, and this induction may be targeted especially on the flavonoid branch.

Stress-induced proteins

Among the six stress-inducing proteins, decreasing abundance in asymptomatic wood of symptomatic plants (A, E), three have already been described in various plant-microbe interactions. The major latex protein (MLP), known to be associated with pathogen defense responses (Osmark *et al.*, 1998), was down-regulated in grapevine leaves following phytoplasma infection (Margaria *et al.*, 2013). An increase of GR-RBP proteins has been reported in pea during *Peronospora viciae* infection, providing evidence of its role in the response of plants to pathogens (Amey *et al.*, 2008). Many studies have reported that 14-3-3 transcripts are accumulated in susceptible and resistant plants affected by pathogenic fungi (Roberts *et al.*, 2002). These proteins may play active roles in defense response by making host cells more resistant to infection and penetration.

Different responses in asymptomatic and BST wood independent of external symptoms

A comparison of protein expression in asymptomatic and BST wood (C1/C2, A1/A2, E1/E2) showed three interesting categories/trends related to the presence or absence of wood and foliar symptoms. In the first category, we observed an increase of protein expression in BST wood with respect to asymptomatic wood (s1105, s1202, s1208, s2211, s2212, s2302, s4216, s4221, s5215, s6002, s7319). The main proteins identified in these spots belonged to the detoxification system (GST, SOD), primary metabolism (GEM-like, transaldolase, endo- β -D-glucanase), stress-induced proteins (14-3-3, RS1, SSP), phenylpropanoid metabolism (CHI, IFR-L4) and PR proteins (TLP). The significant induction of the detoxification system in symptomatic plants confirms its role as a stress marker of GLSD infection (Valtaud *et al.*, 2009), and supports the toxin hypothesis in explaining at least the GLSD symptom development (Magnin-Robert *et al.*, 2011). The strong protein expression from the phenylpropanoid pathway in BST wood is in accordance with the observed accumulation of phenolic compounds (Del Rio *et al.*, 2001). In contrast, the second category was characterized by greater protein expression in asymptomatic wood than in BST wood (s1007, s3105, s3107, s3202, s3203, s4004, s6203, s6420) (Figure 4, Table 1). Most of these proteins were smHSPs, and they could play important defensive roles in the grapevine wood before or at the beginning of extensive fungal colonization. These smHSPs may act as molecular chaperones, resulting in the maintenance of cellular conditions suitable for inducible plant defense responses (Maimbo *et al.*, 2007). The third category was characterized by proteins showing greater expression levels in asymptomatic or BST wood of control plants than in apoplectic and esca proper affected plants (s4212, s5316). The major proteins included in this category belonged to the proteasome activity class, stress-induced proteins (SSP) and isoflavonoid pathway (IFR-L4). This suggests that these proteins may be important for preventing or limiting foliar symptom development.

Different responses in woody tissues correlated to external symptoms

A comparison of protein expression in apoplectic and GLSD affected plants (C1/A1/E1 and C2/

A2/E2) showed three interesting categories/trends related to presence or absence. In the first category, similar responses in A- and E-affected plants were observed, but different to the responses observed for control plants (s1105, s1202, s1208, s2211, s2212, s2302, s4212, s4221, s7210) (Figure 4, Table 1). Most of the proteins were involved in cell rescue and defense and in protein synthesis and degradation. These data suggest that with the development of visual symptoms, common multiple-stress responses were induced in woody tissues, such as the antioxidant defense system, the phenylpropanoid pathway, PR-proteins and activation of protein metabolism. The second category was characterized by reduced protein expression in woody tissues (asymptomatic wood and/or BST) of GLSD-affected plants than in apoplectic plants (s3107, s3202, s3203, s4004, s6001, s6101) (Figure 4, Table 1). Most of these proteins were smHSPs (smHSP chloroplastic and 17.9kDa class HSP). Stress, induced by the development of GLSD-disease, probably damages host capacity to maintain cellular functions in woody tissues. HSPs function may extend beyond their chaperone activity, limiting the damage that results from ROS accumulation (Gurley, 2000). The third category consists of proteins whose expression is less in either asymptomatic wood (s5215, s5316, s5422) or BST wood (s6203, s6420) of apoplectic vines. In both cases, the proteins belong to various categories: cell division (DHFR), cell-wall synthesis (polymyxin resistance protein ARNa), proteins metabolism (60SRP), stress-induced proteins (SSP) and isoflavonoid pathway (IFR-L4). Results suggest that several proteins involved in multiple metabolic pathways were perturbed in lignified tissues during apoplexy development, as well as in the green stems (Spagnolo *et al.*, 2012).

Conclusions

Different quantitative protein expressions were related to the nature of samples. Expression in BST (high rate of GLSD and/or esca agent inoculum) or asymptomatic wood (low or absent inoculum) was more pronounced than that related to the presence or absence of foliar symptoms (apoplexy or GLSD). However, some changes linked to the presence or absence of foliar symptoms were also observed. Results from biological isolation indicated that the inoculum of GLSD agents in the BST wood of symptomatic vines (A and E) is likely to be greater than

in BST wood of control plants. This represents an important association between fungal pathogens and foliar symptom development. Considering that association, a hypothesis could be that quantitative and/or qualitative proteome alterations in the BST wood of plants expressing foliar symptoms are not enough for avoiding their appearance. On the other hand, those proteins over regulated in asymptomatic wood could be regarded as the limiting factor in BST wood for avoiding foliar symptom development. Our results provide evidence of a few different responses in the trunk wood between apoplectic and esca proper affected plants. This could mean that, despite the differences in these external symptoms, grapevine response at trunk wood invasion is very similar. Although these responses can be caused by several different factors, apoplexy especially occurs on plants that have already shown GLSD symptoms at least once. The host response may therefore be simply due to the fact that plants can react in the same way to different stresses, or, at least in the case of GLSD, apoplexy would just represent a different effect provoked by the same cause or causal agents.

Acknowledgements

This research was financed by the national Contract Project État-Région (CPER) program - task E1 altesca and Compte d'Affectation Spéciale au Développement Agricole et Rural (CASDAR). Proteomic studies were supported by the CNRS and the "Agence National de la Recherche" (ANR). The company Moët & Chandon is thanked for making available the vineyard used as the experimental plot in this study.

Literature cited

- Afroz A., G.M. Ali, A. Mir and S. Komatsu, 2011. Application of proteomics to investigate stress-induced proteins for improvement in crop protection. *Plant Cell Reports* 30, 745–763.
- Al-Wahaibi M.H., 2011. Plant heat-shock proteins: a mini review. *Journal of King Saud University* 23, 139–150.
- Amey R.C., T. Schleicher, J. Slinn, M. Lewis, H. McDonald, S.J. Neill and P.T.N. Spencer-Phillips, 2008. Proteomic analysis of a compatible interaction between *Pisum sativum* (pea) and the downy mildew pathogen *Peronospora viciae*. *European Journal of Plant Pathology* 122, 41–55.
- Andolfi, A., L. Mugnai, J. Luque, G. Surico, A. Cimmino and A. Evidente, 2011. Phytotoxins produced by fungi associated with grapevine trunk diseases. *Toxins* 3, 1569–1605.

- Banzet N., C. Richard, Y. Desveaux, M. Kazmaizer, J. Gagnon and C. Triantaphylidès, 1998. Accumulation of small heat shock proteins, including mitochondrial HSP22, induced by oxidative stress and adaptative response in tomato cells. *Plant Journal* 13, 519–527.
- Bélanger R.R., P.D. Manion and D.H. Griffin, 1990. Amino acid content of water-stressed plantlets of *Populus tremuloides* clones in relation to clonal susceptibility to *Hypoxylon mammatum* in vitro. *Canadian Journal of Botany* 68, 26–29.
- Berger S., M. Papadopoulos, U. Schreiber, W. Kaiser and T. Roitsch, 2004. Complex regulation of gene expression, photosynthesis and sugar levels by pathogen infection in tomato. *Physiologia Plantarum* 122, 419–428.
- Bertsch C., M. Ramirez-Suero, M. Magnin-Robert, P. Larignon, J. Chong, E. Abou-Mansour, A. Spagnolo, C. Clément and F. Fontaine, 2013. Trunk diseases of grapevine: complex and still poorly understood syndromes described as eutypa die-back, esca and black dead arm. *Plant Pathology* 62, 243–265.
- Bézier A., B. Lambert and F. Baillieul, 2002. Study of defence-related gene expression in grapevine leaves and berries infected with *Botrytis cinerea*. *European Journal of Plant Pathology* 108, 111–120.
- Camps C., C. Kappel, P. Lecomte, C. Léon, E. Gomès, P. Coutos-Thévenot and S. Delrot, 2010. A transcriptomic study of grapevine (*Vitis vinifera* cv. Cabernet-Sauvignon) interaction with the vascular ascomycete fungus *Eutypa lata*. *Journal of Experimental Botany* 61, 1719–1737.
- Carter M.V., 1994. Wood and root diseases caused by fungi. In: *Compendium of grape diseases* (Pearson, A.C. Goheen, ed.), 3rd ed, APS Press, St-Paul, MN, USA, 32–34.
- Charmont S., E. Jamet, R. Pont-Lezica and H. Canut, 2005. Proteomic analysis of secreted proteins from *Arabidopsis thaliana* seedlings: improved recovery following removal of phenolic compounds. *Phytochemistry* 66, 453–461.
- Crous P.W. and W. Gams, 2000. *Phaeoconiella chlamydospora* gen. et comb. Nov., a causal organism of Petri grapevine decline and esca. *Phytopathologia Mediterranea* 39, 112–118.
- Crous P.W., B. Slippers, M.J. Wingfield, J. Rheeder, W.F.O. Marasas, A.J.L. Phillips, A. Alves, T. Burgess, P. Barber and J.Z. Groenewald, 2006. Phylogenetic lineages in the Botryosphaeriaceae. *Studies in Mycology* 55, 235–253.
- Del Rio J.A., A. Gonzalez, M.D. Fuster, J.M. Botia, P. Gomez, V. Frias and A. Ortuño, 2001. Tylose formation and changes in phenolic compounds of grape roots infected with *Phaeoconiella chlamydospora* and *Phaeoacremonium* species. *Phytopathologia Mediterranea* 40, 394–399.
- Deuschle K., D. Funck, G. Forlani, H. Stransky, A. Biehl, D. Leister, E. Vand der Graff, R. Kunze, and W.B. Frommer, 2004. The role of [Delta]1-pyrrolidone-5-carboxylate dehydrogenase in proline degradation. *Plant Cell* 16, 3413–3425.
- Dixon R.A., L. Achnine, P. Kota, C.J. Liu, M.S.S. Reddy and L. Wang, 2002. The phenylpropanoid pathway and plant defence—a genomics perspective. *Molecular Plant Pathology* 3, 371–390.
- Ehness R., M. Ecker, D.E. Godt and T. Roitsch, 1997. Glucose and stress independently regulate source and sink metabolism and defense mechanisms via signal transduction pathways involving protein phosphorylation. *Plant Cell* 9, 1825–1841.
- Elias J. E. and S.P. Gygi, 2007. Target-decoy search strategy for increased confidence in large-scale protein identifications by mass spectrometry. *Nature Methods* 4, 207–214.
- Essakhi S., L. Mugnai, P.W. Crous, J.Z. Groenewald and G. Surico, 2008. Molecular and phenotypic characterization of novel *Phaeoacremonium* species isolated from esca diseased grapevines. *Persoonia* 21, 119–134.
- Figueiredo A., A.M. Fortes, S. Ferreira, M. Sebastiana, Y.H. Choi, L. Sousa, B. Acioli-Santos, F. Pessoa, R. Verpoorte and M.S. Pais, 2008. Transcriptional and metabolic profiling of grape (*Vitis vinifera* L.) leaves unravel possible innate resistance against pathogenic fungi. *Journal of Experimental Botany* 59, 3371–3381.
- Fischer M.A., 2002. A new wood-decaying basidiomycete species associated with esca of grapevine: *Fomitiporia mediterranea* (Hymenochaetales). *Mycological Progress* 1, 315–324.
- Frova C., 2003. The plant glutathione transferase gene family: genomic structure, functions, expression and evolution. *Physiologia Plantarum* 119, 469–479.
- Fung R.W.M., M. Gonzalo, C. Fekete, L.G. Kovacs, Y. He, E. Marsch, L.M. McIntyre, D.P. Schachtman and W. Qiu, 2008. Powdery mildew induces defence-oriented reprogramming of the transcriptome in a susceptible but not in a resistant grapevine. *Plant Physiology* 146, 236–249.
- Fussler L., N. Kobes, F. Bertrand, M. Mauray, J. Grosman and S. Savary, 2008. A characterisation of grapevine trunk diseases in France from data generated by the National Grapevine Wood Survey. *Phytopathology* 98, 571–579.
- Golkari S., J. Gilbert, S. Prashar and J.D. Procnier, 2007. Microarray analysis of *Fusarium graminearum*-induced wheat genes: identification of organ-specific and differentially expressed genes. *Plant Biotechnology Journal* 5, 38–49.
- Görg A., W. Postel, J. Weser, S. Günther, J.R. Strahler, S.M. Hanash, and L. Somerlot, 1987. Elimination of point streaking on silver stained two-dimensional gels by addition of iodoacetamide to the equilibration buffer. *Electrophoresis* 8, 122–124.
- Guillen P., M. Guis, G. Martinez-Reina, S. Colrat, S. Dalmeyrac, M. Bouzayen, J.-P. Roustan, J. Fallot, J.-C. Pech and A. Latché, 1998. A novel NADPH-dependent aldehyde reductase gene from *Vigna radiata* confers resistance to the grapevine fungal toxin eutypine. *Plant Journal* 16, 335–343.
- Gurley W.B., 2000. HSP101: a key component for the acquisition of thermotolerance in plants. *Plant Cell* 12, 457–460.
- Herbers K., P. Meuwly, W.B. Frommer, J.-P. Métraux and C. Sonnwald, 1996. Systemic acquired resistance mediated by the ectopic expression of invertase: possible hexose sensing in the secretory pathway. *Plant Cell* 8, 793–803.
- Kim M., J.H. Lim, C.S. Ahn, K. Park, G.T. Kim, W.T. Kim and H.S. Pai, 2006. Mitochondria-associated hexokinases play a role in the control of programmed cell death in *Nicotiana benthamiana*. *Plant Cell* 18, 2341–2355.
- Ko J.-H., K.-H. Han, S. Park and J. Yang, 2004. Plant body weight-induced secondary growth in *Arabidopsis* and its transcription phenotype revealed by whole-transcriptome profiling. *Plant Physiology* 135, 1069–1083.
- Kuntzmann P., S. Villaume, P. Larignon and C. Bertsch, 2010. Esca, BDA and Eutypiosis: foliar symptoms, trunk lesions and fungi observed in diseased vinestocks in two vine-

- yards in Alsace. *Vitis* 49, 71–76.
- La Camera S., G. Gouzerth, S. Dhondt, L. Hoffmann, B. Fritig, M. Legrand and T. Heitz, 2004. Metabolic reprogramming in plant innate immunity: the contributions of phenylpropanoid and oxylipin pathways. *Immunological Reviews* 198, 267–284.
- Larignon P., F. Fontaine, S. Farine, C. Clément and C. Bertsch, 2009. Esca et Black Dead Arm: deux acteurs majeurs des maladies du bois chez la vigne. *Comptes Rendus de l'Académie des Sciences Biologie* 332, 765–783.
- Letousey P., F. Baillieul, G. Perrot, C. Rabenoelina, M. Boulay, N. Vaillant-Gaveau, C. Clément and F. Fontaine, 2010. Early events prior to visual symptoms in apoplectic form of esca disease. *Phytopathology* 100, 424–431.
- Lima M.R.M., F. Ferreres and A.C.P. Dias, 2012. Response of *Vitis vinifera* cell cultures to *Phaeoemoniella chlamydospora*: changes in phenolic production, oxidative state and expression of defence-related genes. *European Journal of Plant Pathology* 132, 133–146.
- Magnin-Robert M., P. Letousey, A. Spagnolo, C. Rabenoelina, L. Jacquens, L. Mercier, C. Clément and F. Fontaine, 2011. Leaf stripe form of esca induces alteration of photosynthesis and defence reactions in presymptomatic leaves. *Functional Plant Biology* 38, 856–866.
- Maimbo M., K. Ohnishi, Y. Hikichi, H. Yoshioka and A. Kiba, 2007. Induction of a small heat shock protein and its functional roles in *Nicotiana* plants in the defence response against *Ralstonia solanacearum*. *Plant Physiology* 145, 1588–1599.
- Margarita P. and S. Palmano, 2011. Response of the *Vitis vinifera* L. cv. 'Nebbiolo' proteome to Flavescence dorée phytoplasma infection. *Proteomics* 11, 212–214.
- Margarita P., S. Abbà and S. Palmano, 2013. Novel aspects of grapevine response to phytoplasma infection investigated by a proteomic and phospho-proteomic approach with data integration into functional networks. *BMC Genomics* 14, 38–52.
- Mitchell H., M. Ayliffe, K. Rashid and A. Pryor, 2006. A rust-inducible gene from flax (*fls1*) is involved in proline catabolism. *Planta* 23, 213–222.
- Monteiro S., M. Barakat, M.A. Piçarra-Pereira, A.R. Teixeira and R.B. Ferreira, 2003. Osmotin and thaumatin from grape: a putative general defense mechanism against pathogenic fungi. *Phytopathology* 93, 1505–1512.
- Mugnai L., A. Graniti and G. Surico, 1999. Esca (black meales) and brown wood-streaking: two old and elusive diseases in grapevines. *Plant Disease* 83, 404–418.
- Osmark P., B. Boyle and N. Brisson, 1998. Sequential and structural homology between intracellular pathogenesis-related proteins and a group of latex proteins. *Plant Molecular Biology* 38, 1243–1246.
- Petit A.N., N. Vaillant, M. Boulay, C. Clément and F. Fontaine, 2006. Alteration of photosynthesis in grapevines affected by esca. *Phytopathology* 96, 1060–1066.
- Phillips A.J.L., 2002. *Botryosphaeria* species associated with diseases of grapevines in Portugal. *Phytopathologia Mediterranea* 41, 3–18.
- Polesani M., F. Desario, A. Ferrarini, A. Zamboni, M. Pezzoti, A. Kortekamp and A. Polverari, 2008. cDNA-AFLP analysis of plant and pathogen genes expressed in grapevine with *Plasmopara viticola*. *BMC Genomics* 9, 142–155.
- Roberts M.R., J. Salinas and D.B. Collinge, 2002. 14-3-3 proteins and the response to abiotic and biotic stress. *Plant Molecular Biology* 50, 1031–1039.
- Roje S., 2006. S-Adenosyl-L-methionine: beyond the universal methyl group donor. *Phytochemistry* 67, 1686–1698.
- Spagnolo A., G. Marchi, F. Peduto, A.J.L. Phillips and G. Surico, 2011. Detection of Botryosphaeriaceae species within grapevine woody tissues, with particular emphasis on the *Neofusicoccum parvum*/N. *ribis* complex. *European Journal of Plant Pathology* 129, 485–500.
- Spagnolo A., M. Magnin-Robert, T.D. Alayi, C. Cilindre, L. Mercier, C. Schaeffer-Reiss, A. Van Dorsseleer, C. Clément and F. Fontaine, 2012. Physiological changes in green stems of *Vitis vinifera* L. cv. Chardonnay in response to esca proper and apoplexy revealed by proteomic and transcriptomic analyses. *Journal of Proteome Research* 11, 461–475.
- Surico G., 2009. Towards a redefinition of the diseases within the esca complex of grapevine. *Phytopathology Mediterranea* 48, 5–10.
- Surico G., L. Mugnai and G. Marchi, 2008. The esca disease complex. In: *Integrated management of diseases caused by fungi, phytoplasma and bacteria*. (A. Ciancio, K.G. Mukerji, K.J. ed.), Springer, Dordrecht, Netherlands, 119–136.
- Suty L., J. Lequeu, A. Lançon, P. Etienne, A.S. Petitot and J.P. Blein, 2003. Preferential induction of 20S proteasome subunits during elicitation of plant defence reactions: towards the characterization of « plant defence proteasomes ». *The International Journal of Biochemistry and Cell Biology* 35, 637–650.
- Valtaud C., C.H. Foyer, P. Fleurat-Lessard and A. Bourbouloux, 2009. Systemic effects on leaf glutathione metabolism and defence protein expression caused by esca infection in grapevines. *Functional Plant Biology* 36, 260–279.
- Vanderauwera S., P. Zimmermann, S. Rombauts, S. Vandenaebelle, C. Langebartels, W. Gruissem, D. Inzé and F. Van Breusegem, 2005. Genome-wide analysis of hydrogen peroxide regulated gene expression in Arabidopsis reveals a high light-induced transcriptional cluster involved in anthocyanin biosynthesis. *Plant Physiology* 139, 806–821.
- Vizcaíno J.A., R. Côté, F. Reisinger, H. Barsnes, J.M. Foster, J. Rameseder, H. Hermjakob and L. Martens, 2010. The Proteomics Identifications database: 2010 update. *Nucleic Acids Research* 38, D736–D742.
- Yang L., H. Lin, Y. Takahashi, F. Chen, M.A. Walker and E.I. Civerolo, 2011. Proteomic analysis of grapevine stem in response to *Xylella fastidiosa* inoculation. *Physiological and Molecular Plant Pathology* 75, 90–99.